Geotech Geol Eng (2019) 37:5441–5455
https://doi.org/10.1007/s10706-019-00991-1

ORIGINAL PAPER

Practical Use of Modified Hoek–Brown Criterion for Soil Slope Stability Analysis

Daniel R. VandenBerge · Michael P. McGuire

Received: 13 March 2019 / Accepted: 16 June 2019 / Published online: 20 June 2019

Abstract Many slopes are comprised of soils that exhibit a nonlinear shear strength or failure envelope, and multiple mathematical relationships have been developed to account for this nonlinearity. At the same time, the numerical shear strength reduction (SSR) method has become a common method for analyzing the stability of slopes. Despite these developments, a practical, commercially available method to include nonlinear shear strength in numerical analysis has not been established for soil. The Generalized Hoek–Brown (GHB) model provides a nonlinear failure criterion, but is formulated for use with rock. This paper proposes a Modified Hoek–Brown (MHB) criterion to make the model applicable to soil and leverage the GHB criterion present in many numerical analysis packages. Past applications of SSR to the GHB are discussed and a numerical method for reduction of the parameters in the context of soil slopes is proposed. A simple wedge analysis validates the MHB method for a linear envelope. Three examples of increasing complexity compare results of limit equilibrium with both finite element and finite difference SSR analyses. In general, the different numerical methods yield very similar results. The SSR method using MHB predicts critical strength reduction factors 2–5% lower than the limit equilibrium factors of safety. The approach presented in this paper allows practitioners to model nonlinear shear strength in finite element strength reduction analysis for cases where this nonlinearity is judged to be an important factor.

Keywords Hoek Brown · Nonlinear · Shear strength reduction · Slope stability · Finite element · Finite difference

D. R. VandenBerge (✉)
Tennessee Technological University,
Box 5015, Cookeville, TN 38505, USA
e-mail: dvandenberge@tntech.edu

M. P. McGuire
Lafayette College, 740 High Street, Easton, PA 18042, USA
e-mail: mcguirem@lafayette.edu

List of Symbols

σ'_{1f}	Major principal effective stress at failure
σ'_{3f}	Minor principal effective stress at failure
σ'_{ci}	Unconfined compressive strength of rock for GHB envelope
m_b	Dimensionless slope parameter for the GHB envelope
s	Normalized tensile strength parameter for the GHB envelope
A	Curvature exponent for the GHB envelope
P_a	Normalization stress equal to atmospheric pressure
a	Dimensionless slope parameter for the MHB envelope
b	Curvature exponent for the MHB envelope
t	Normalized tensile strength parameter for the MHB envelope

F	Factor of safety = ratio of shear strength to shear stress required for stability
σ'_{ff}	Effective normal stress at failure on the failure plane
τ_{ff}	Shear stress at failure on failure plane = full shear strength
ϕ'	Effective friction angle for a linear envelope
c'	Effective stress cohesion intercept for linear envelope
SRF	Strength reduction factor, subscript "crit" indicates the critical value
ϕ'_i	Instantaneous effective friction angle defined by the first derivative of the strength envelope
c'_i	Cohesion intercept for instantaneous linear envelope
K_p	Principal stress ratio
$\phi'_{i,red}$	Instantaneous effective friction angle reduced by the SRF
$c'_{i,red}$	Cohesion intercept for instantaneous linear envelope reduced by the SRF
$\sigma'_{1f,red}$	Major principal effective stress at failure corresponding to the reduced MHB envelope
$\sigma'_{3f,red}$	Minor principal effective stress at failure corresponding to the reduced MHB envelope
$\tau_{ff,red,k}$	Shear stress at failure on failure plane reduced by SRF (k = index)
a_{adj}	Slope parameter fit to the reduced MHB envelope
b_{adj}	Curvature exponent fit to the reduced MHB envelope
t_{adj}	Normalized tensile strength parameter fit to the reduced MHB envelope
$\sigma'_{ff,adj,k}$	Effective normal stress at failure on the failure plane reduced by SRF (k = index)
$\tau_{ff,adj,k}$	Shear stress at failure on failure plane reduced by SRF (k = index)
K	Ratio of minor to major effective principal stress
α	Slip surface angle above horizontal
a_{PF}	Slope parameter for two parameter power function
b_{PF}	Curvature exponent for two parameter power function

1 Introduction

Practical methods for slope stability analysis using finite element and finite difference methods, such as shear strength reduction (SSR) analysis (Griffiths and Lane 1999), have become fairly well established in geotechnical engineering. These numerical methods are attractive because they do not require a priori assumptions about the shape or location of the failure surface, or the inclination of interslice forces. The type of search used in LE analysis and the permissible shape of the slip surface (e.g., circular vs noncircular) can have significant impacts on the resultant calculated factor of safety (e.g., Baker 1980; Greco 1996; Cheng 2003). In certain situations, the critical failure mechanism is complex and is very difficult to find or represent using conventional LE analysis, even if a robust search algorithm is used and noncircular failure surfaces are considered. The analysis of the downstream slope of Oroville Dam provided herein is an example of this phenomenon. Other published examples of complex failure surfaces that are difficult to analyze or represent using conventional LE procedures include the stability of embankment slopes supported on columns or deep mixed panels, which can fail by tilting or bending (Navin and Filz 2006), reinforced slopes (Pockoski and Duncan 2000), and slopes with multiple soil and rock layers (e.g., Ching et al. 2010; Leshchinsky and Ambauen 2015). In situations where complex failure mechanisms are suspected, SSR and LE analyses can be used to cross check the results of the slope stability analysis since there are limitations associated with each method (Cheng et al. 2007).

The shear strength of soil and rock materials is frequently characterized using a normal stress dependent strength envelope. Linear forms such as the Mohr–Coulomb (MC) strength equation are often adequate for slope stability analyses; however, it is well understood that strength envelopes often exhibit nonlinearity, especially if a large range of stresses exist in the slope under consideration. The primary reasons for nonlinearity in sands, gravels, and rockfill are decreasing rates of dilation and increasing tendency for particle fracture with increasing normal stress (Lee and Seed 1967; Marachi et al. 1972). In silts and clays, nonlinearity in the strength envelope is attributed to increased tendency for preferential particle alignment with increasing normal stress (Mesri

and Shahien 2003). Nonlinearity in the strength envelope can have a significant impact on the results of slope stability analyses (e.g., Jiang et al. 2003; VandenBerge et al. 2013; Castellanos et al. 2016a, b; VandenBerge et al. 2019), particularly for shallow failures. Therefore, situations arise that require the use of piecewise linear or nonlinear mathematical forms to represent the strength envelope.

Many commercial LE analysis codes allow the analyst to specify a piecewise linear or nonlinear form, such as a power function, for the strength equation; however, the availability of piecewise or nonlinear forms in commercial codes that enable SSR analysis remains elusive. One notable exception is the Generalized Hoek–Brown (GHB) failure criterion that is commonly used to represent the stress-dependent shear strength of rock. Some commercial codes perform automatic SSR analysis for GHB materials, while others do not. As discussed later in the paper, some commercial codes that perform automatic strength reduction are formulated specifically for rock in that they are explicitly linked to the Geologic Strength Index (GSI), which is a parameter that is not applicable to soils. The underlying assumption of rock-like behavior prevents the GHB criterion from being practically applied to soils.

The primary aims of this paper are (1) to demonstrate that the GHB failure criterion can be modified to allow application to soils and (2) to describe a procedure for strength reduction of the GHB parameters for situations when automatic routines are not available. This paper provides theoretical validation and three examples of the method's application to soil, comparing the results of the numerical analysis to those from limit equilibrium.

2 Background

2.1 Generalized and Modified Hoek–Brown Failure Criteria

Hoek and Brown (1980) proposed a nonlinear failure criterion for use in rock stability problems that was stated in terms of principal stresses at failure and was ideal for numerical analysis. Hoek and Brown also proposed an accompanying power function relationship that related shear strength to normal stress on a failure plane. This latter relationship appears to have evolved into the three-parameter power function presented by Jiang et al. (2003). Hoek and Brown's two representations of the failure criterion for rock can be fit to the same data but cannot be explicitly derived from one another.

More recently, the Generalized Hoek–Brown equation has become a popular method to describe the failure criterion of rock. The unconfined compressive strength of the rock, σ'_{ci}, dominates the shear strength in many cases and is used as a basis for the GHB envelope. The envelope as defined by Hoek et al. (2002) is

$$\sigma'_{1f} = \sigma'_{3f} + \sigma_{ci}\left(m_b \frac{\sigma'_{3f}}{\sigma_{ci}} + s\right)^A \quad (1)$$

where m_b is a measure of the slope of the envelope, s is a measure of the tensile strength, and A is an exponent that defines the envelope curvature. These three parameters are typically estimated from the Geological Strength Index (GSI) as described in Hoek et al. (2002).

VandenBerge et al. (2019) adopted a modified set of notation and suggested that the GHB equation could be used to represent the shear strength envelope of the soil in terms of effective stress. Since the effective stress shear strength of soil is not dominated by its unconfined strength, VandenBerge et al. (2019) recognized that σ'_{ci} serves the purpose of a normalizing stress in Eq. 1 and can be replaced with atmospheric pressure, P_a, yielding

$$\sigma'_{1f} = \sigma'_{3f} + P_a\left(a \frac{\sigma'_{3f}}{P_a} + t\right)^b \quad (2)$$

This modified from of the GHB equation is referred to herein as the Modified Hoek–Brown (MHB) criterion. Equation 2 utilizes the same mathematical form as Eq. 1, and thereby it can be used directly in finite element and finite difference programs that incorporate GHB. However the equation parameters a, t, and b must be found by regression to laboratory shear strength data and cannot be found from the empirical relationship to GSI used for the corresponding GHB parameters.

The MHB a parameter controls the overall slope of the shear strength envelope while the t parameter is a normalized tensile strength intercept. The b parameter controls the curvature of the shear strength envelope.

2.2 Factors of Safety and Shear Strength Reduction Analysis

As pointed out by past researchers (Hammah et al. 2005; Fu and Liao 2010) the definition of factor of safety must be examined when using the GHB failure criterion for finite element shear strength reduction (SSR) analysis. By comparison, this is also true for the MHB failure criterion. The traditional definition of factor of safety, F, for slope stability is

$$F = \frac{\text{Shear strength}}{\text{Shear stress required for stability}} \tag{3}$$

The denominator, or shear stress required for stability, is determined from statics and simple assumptions for limit equilibrium or statics and constitutive behavior for numerical analysis. The factor of safety is either explicitly or iteratively determined by dividing the shear strength by F until Eq. 3 is satisfied for a given set of constraints. When the strength envelope is defined in terms of effective normal stress and limiting shear stress on the failure surface, as is typical when applying the MC failure criterion, calculation of the reduced shear strength, $\tau_{ff,red}$, is calculated directly by

$$\tau_{\text{ff,red}} = \frac{c'}{F} + \sigma'_{ff}\frac{\tan\phi'}{F} \tag{4}$$

The same approach can be used for any mathematical representation of the failure envelope that directly relates shear strength to effective normal stress on the failure plane.

The shear strength reduction approach uses the same principle within the context of finite element analysis (e.g., Griffiths and Lane 1999). Unlike limit equilibrium, SSR does not explicitly consider a failure surface on which the normal stress can be determined. Rather SSR employs an iterative process of changing the shear strength via changes to the shear strength parameters. For a MC envelope factored by a given strength reduction factor (SRF), the reduced shear strength parameters are $c'_{red} = c'/SRF$ and $\phi'_{red} = \tan^{-1}(\tan\phi'/SRF)$. The numerical model is analyzed repeatedly for a range of SRF values. The critical value, SRF_{crit}, is the highest SRF at which the numerical model remains stable. As mentioned later, model stability is usually assessed using a force or energy convergence criterion or by nodal displacements. In practice, SRF_{crit} is typically treated as equivalent to the factor of safety and is frequently compared to the factor of safety computed by limit equilibrium analysis.

2.3 GHB and Shear Strength Reduction Analysis

The GHB (Eq. 1) and MHB (Eq. 2) failure criteria are defined in terms of principal stresses, which is advantageous for numerical analysis. However, as a result of the nonlinearity of these criteria, an appropriately reduced failure envelope is not produced by simply dividing the model parameters (e.g., m_b or t) by SRF. In other words, reduction of the model parameters by SRF does not result in shear strengths that are also reduced by SRF. Recognizing this difficulty, a variety of numerical approaches have been suggested for employing the GHB equation in SSR analyses of rock (e.g., Hammah et al. 2005; Fu and Liao 2010; Dawson et al. 2000; Shukha and Baker 2003; Shen et al. 2012; Lee and Bobet 2014; Ledesma et al. 2016; Chen et al. 2018). These methods derive expressions for instantaneously-equivalent MC strength parameters (ϕ'_i, c_i) and/or the stress pairs (σ'_{ff}, τ_{ff}) on the strength envelope as a function of σ'_{3f} and the GHB envelope parameters. While different in form, the expressions derived in these studies are mathematically equivalent. Some of the methods differ in how strength reduction is performed. Some methods factor the instantaneous linear envelopes (e.g.Fu and Liao 2010) while other methods define reduced GHB parameters based on the SRF (Hammah et al. 2005). Other differences among SSR methods implemented for the GHB model have been attributed to the choice of flow rule used within the SSR analysis to determine plastic strains (Ledesma et al. 2016).

2.3.1 Instantaneous Linear Envelopes

The predominant approach to shear strength reduction with GHB has been to define instantaneous linear envelopes tangent to the curved failure envelope with parameters ϕ'_i and c'_i as shown in Fig. 1. Dawson et al. (2000), Fu and Liao (2010), Shen et al. (2012), Lee and Bobet (2014) and Chen et al. (2018) derive equivalent equations for instantaneous linear strength parameters and shear and normal stress on the failure plane in terms of σ'_{3f} and GHB parameters. Fu and Liao (2010) explain the iterative process of computing instantaneous strength parameters for each element in a model

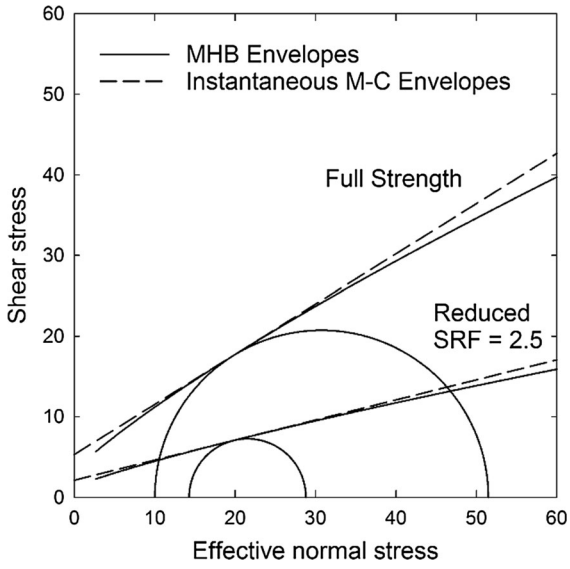

Fig. 1 Instantaneous Mohr–Coulomb Envelope from MHB

based on the stress state from the previous step in the analysis, factoring the MC parameters by the *SRF* in the current step, and then performing elasto-plastic analysis to update the stress state of each element for the next step. For each step in the analysis, a single value of *SRF* is applied to all elements, which will yield different instantaneous MC parameters for elements with different stress states provided that the GHB parameters introduce nonlinearity (i.e. $A < 1$). The explicit finite difference code FLAC (Itasca 2016) used within this study automatically performs strength reduction for the GHB model using instantaneous MC parameters within a process like the one described by Fu and Liao (2010). If the code does not perform this type of strength-reduction automatically, this process can only be utilized in numerical analysis programs that allow in-depth user control of the constitutive model. Users must also be comfortable with programming their own routines within their numerical modeling software. One attractive feature of this type of approach that permits application to soils is that there is no underlying assumption of rock-like properties linked to GSI, unlike the GHB envelope reduction method proposed by Hammah et al. (2005).

In the context of soils, one way to compute the instantaneous MC parameters and stresses on the failure plane is to use the MC relation of principal stresses at failure

$$\sigma'_{1f} = \sigma'_{3f} K_p + 2c'_i \sqrt{K_p} \tag{5}$$

where c'_i is the intercept of the instantaneous linear envelope and K_p is the principal stress ratio determined by the instantaneous friction angle, in degrees, according to

$$K_p = \tan^2\left(45 + \frac{\phi'_i}{2}\right) \tag{6}$$

Equating the first derivatives of Eqs. 2 and 5 with respect to σ'_{3f} reveals that

$$K_p = 1 + ab\left(a\frac{\sigma'_{3f}}{P_a} + t\right)^{b-1} \tag{7}$$

Combining Eqs. 6 and 7, the instantaneous friction angle, in degrees, can be determined for any minor principal stress as

$$\phi'_i = 2\tan^{-1}\left(\sqrt{1 + ab\left(a\frac{\sigma'_{3f}}{P_a} + t\right)^{b-1}}\right) - 90 \tag{8}$$

Similarly it can be shown that the instantaneous cohesion intercept at any σ'_{3f} equals

$$c'_i = \frac{P_a\left(a\frac{\sigma'_{3f}}{P_a} + t\right)^{b} - \sigma'_{3f} ab\left(a\frac{\sigma'_{3f}}{P_a} + t\right)^{b-1}}{2\sqrt{1 + ab\left(a\frac{\sigma'_{3f}}{P_a} + t\right)^{b-1}}} \tag{9}$$

From the instantaneous friction angle, the stress pair (σ'_{ff}, τ_{ff}) corresponding to the failure plane can be calculated as

$$\begin{aligned}\sigma'_{ff} &= \left(\frac{\sigma'_{1f} + \sigma'_{3f}}{2}\right) - \left(\frac{\sigma'_{1f} - \sigma'_{3f}}{2}\right)\sin\phi'_i \\ &= \left(\frac{\sigma'_{1f} + \sigma'_{3f}}{2}\right) - \left(\frac{\sigma'_{1f} - \sigma'_{3f}}{2}\right)\frac{K_p - 1}{1 + K_p}\end{aligned} \tag{10}$$

$$\tau_{ff} = \frac{\sigma'_{1f} - \sigma'_{3f}}{2}\cos\phi'_i = \left(\sigma'_{1f} - \sigma'_{3f}\right)\frac{\sqrt{K_p}}{1 + K_p} \tag{11}$$

2.3.2 Reduced GHB Envelope

The approach proposed by Hammah et al. (2005) finds a strength envelope of τ_{ff} versus σ'_{ff} using expressions solely in terms of σ'_{3f} and the GHB envelope parameters. For the same inputs, the normal and shear stresses found by Hammah et al. are equivalent to those found by Eqs. 10 and 11. After the shear strength

envelope has been determined for a range of normal stresses, the values of τ_{ff} are divided by the desired *SRF* to calculate a reduced failure envelope in keeping with Eq. 3. Next, Hammah et al. use a numerical scheme to find a reduced set of GHB parameters that produces a failure envelope equivalent to the reduced failure envelope. Hammah et al.'s scheme to find reduced GHB parameters focuses on reduction of σ'_{ci} because this parameter dominates the shear strength of rock in the model. The reduced forms of A, m_b, and s are found by varying the geological strength index, *GSI*, and the intact rock material property, m_i, in conformance with the GHB model described in Hoek et al. (2002). The Hammah et al. approach ensures the reduced model parameters conform to typical rock behavior, but restricts the flexibility of the failure criterion to apply to other materials, such as soil.

3 Proposed SSR Method for Soil Using MHB

The following method leverages the instantaneous linear envelope concept to define a reduced MHB envelope for a particular strength reduction factor, *SRF*. The adjusted MHB parameters can be used as part of a shear strength reduction analysis even for software that does not have an appropriate automatic routine or advanced user-defined functions.

1. Select an appropriate range of effective minor principal stresses for each problem as part of the SSR process. A logical approach is to use a range likely starting at a minor principal effective stress of zero and extending to at least as large as that predicted by an unfactored finite element analysis of the problem.
2. For each value of σ'_{3f}, calculate the corresponding value of σ'_{1f} using Eq. 2 with the unfactored MHB parameters. Also calculate the instantaneous values of ϕ'_i and c'_i from Eqs. 8 and 9, and the stress pair (σ'_{ff}, τ_{ff}) on the MC envelope from Eqs. 10 and 11.
3. The instantaneous friction angle and cohesion intercept can be used with the typical strength reduction approach, producing reduced values of

$$\phi'_{i,red} = \tan^{-1}\left(\frac{\tan\phi'_i}{SRF}\right) \tag{12}$$

$$c'_{i,red} = \frac{c'_i}{SRF} \tag{13}$$

4. Using the reduced Mohr–Coulomb parameters, the reduced shear strength, $\tau_{ff,red}$, can be calculated for each value of σ'_{3f} as

$$\tau_{ff,red} = \frac{\tau_{ff}}{SRF} = c'_{i,red} + \sigma'_{ff}\tan\phi'_{i,red} \tag{14}$$

where σ'_{ff} is the effective normal stress on the failure plane corresponding to each unreduced value of σ'_{3f} (i.e. at *SRF* equal to unity).

5. Reduction of the failure envelope causes the Mohr circle corresponding to σ'_{ff} to also reduce in size as illustrated in Fig. 1. The value of $\sigma'_{3f,red}$ for the reduced Mohr circle is

$$\sigma'_{3f,red} = \sigma'_{ff} + \tau_{ff,red}\frac{\sin\phi'_{i,red} - 1}{\cos\phi'_{i,red}} \tag{15}$$

6. In order to determine adjusted MHB parameters that most closely fit to the reduced shear strength envelope defined by stress pairs (σ'_{ff}, $\tau_{ff,red}$), an iterative minimization process is required as follows.
   - 6a. Select an initial set of MHB parameters (a_{adj}, b_{adj}, and t_{adj}) that can be adjusted to fit the reduced shear strength envelope. By default, begin with adjusted parameters equal to the unreduced parameters.
   - 6b. Calculate values of $\sigma'_{1f,red}$ from Eq. 2 based on the $\sigma'_{3f,red}$ value and the adjusted MHB parameters.
   - 6c. Next, calculate the adjusted values of $\sigma'_{ff,adj}$ and $\tau_{ff,adj}$ using Eqs. 10 and 11 along with the reduced principal stresses and shear parameters
7. Finally, employ any method that reduces the error between the reduced shear strength envelope and the adjusted MHB envelope. One way to consider this error is to numerically calculate the area between the two envelopes. For adjacent calculation points, the integrated error is

$$\varepsilon_k = \left|\frac{1}{4}\left(\frac{\tau_{ff,red,k} - \tau_{ff,adj,k}}{2} + \frac{\tau_{ff,red,k-1} - \tau_{ff,adj,k-1}}{2}\right) \times \left(\frac{\sigma'_{ff,k} - \sigma'_{ff,k-1}}{2} + \frac{\sigma'_{ff,adj,k} - \sigma'_{ff,adj,k-1}}{2}\right)\right| \tag{16}$$

7a. The total error for a trial set of adjusted MHB parameters is found by summing ε_k over the full range of stress considered in the fitting process.

7b. The adjusted MHB envelope that best fits the reduced strength envelope is found by iteratively changing a_{adj}, b_{adj}, and t_{adj} and repeating Steps 6 and 7 until the total error is minimized.

The process described in Steps 1–7 must be performed for every trial value of *SRF*. The adjusted MHB parameters are then used in individual finite element analyses, following the same procedure as a typical shear strength reduction analysis. The critical *SRF* is selected as the highest value at which the model converges.

The proposed approach could also be implemented within limit equilibrium analysis to apply the MHB criterion. However, many other nonlinear failure envelopes are available, which define shear strength directly as a function of effective normal stress (e.g., VandenBerge et al. 2019). For this reason, other failure envelope forms are more conducive for representing soil in limit equilibrium.

4 Validation

The application of the MHB envelope to soil slope stability problems is validated here for a cohesionless material having a Mohr–Coulomb envelope with constant ϕ'. In this case, the MHB parameter values become, $a = K_p - 1$, $t = 0$, and $b = 1$. Values of normal and shear stress at failure can solved for as a function of the minor principal stress at failure and the MHB parameter a according to Eqs. 10 and 11, which simplify to Eqs. 17 and 18.

$$\sigma'_{ff} = \frac{\sigma'_{3f}}{2}\left[(2+a) - \frac{a^2}{2+a}\right] \tag{17}$$

$$\tau_{ff} = \sigma'_{3f}\left[\frac{a\sqrt{1+a}}{2+a}\right] \tag{18}$$

In this case, τ_{ff} is proportional to σ'_{ff} according to tan ϕ', and strength reduction of MHB parameters by the factor of safety can be performed explicitly by

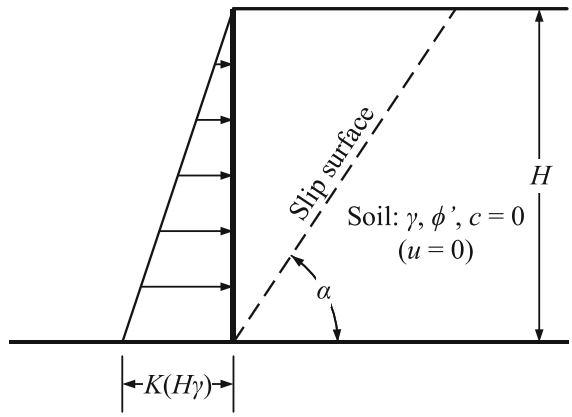

Fig. 2 Vertical cut in soil supported by triangular pressure distribution

$$\frac{a_{red}}{\sqrt{1+a_{red}}} = \frac{a}{F\sqrt{1+a}} \tag{19}$$

while t and b remain fixed at their original values of 0 and 1, respectively.

Figure 2 shows a vertical cut in cohesionless soil with zero pore pressure that is supported by a triangular pressure distribution that is proportional to the vertical stress according to the lateral earth pressure coefficient, K. Under these conditions, which are consistent with level cohesionless backfill behind a vertical smooth wall, the critical slip surface is planar (Xie and Leshchinsky 2016).

The ratio of principal stresses in the soil for any value of K within the limits of $0 < K < 1$ is equal to

$$\frac{\sigma'_3}{\sigma'_1} = K = \frac{1}{(1+a_{red})} \tag{20}$$

The factor of safety against shearing along the critical slip surface for the stress conditions imposed by overburden and the applied lateral pressure is equal to

$$F = \frac{(K_p - 1)\sqrt{\frac{1}{K}}}{\left(\frac{1}{K} - 1\right)\sqrt{K_p}} \tag{21}$$

which is found by combining Eqs. 19 and 20 and substituting $K_p - 1$ for a.

For a soil having a friction angle equal to 37°, the factor of safety found using Eq. 21 equals 1.58 for the case where the pressure distribution is equivalent to an at-rest condition (i.e. $K = K_o \approx 1 - \sin\phi'$), while the

factor of safety equals 1.00 for an active condition (i.e. $K = 1/K_p$).

The results can be confirmed by a simple wedge analysis, where the shear strength along the sliding surface of the wedge is characterized using a conventional Mohr–Coulomb strength envelope. The factor of safety of a supported wedge inclined at an angle α above horizontal (Fig. 2) is found according to

$$F = \frac{(\cot \alpha + K \tan \alpha) \tan \phi'}{(1 - K)} \quad (22)$$

The critical factor of safety is found through a minimization process of Eq. 22 for trial values of α. The same factors of safety for the at-rest and active pressure distributions are obtained using wedge analysis with a Mohr–Coulomb strength envelope as those obtained using the explicit solution based on a linear MHB strength envelope.

5 Comparison to Other Methods

Three comparative examples with increasing complexity have been selected to demonstrate the applicability of this method. Rather than providing formal validation, these examples are cross-checks showing that reasonably similar results are obtained when the soil is represented by MHB parameters compared to other methods. The first example is a simple slope described by Griffiths and Lane (1999) that is comprised of soil with a linear Mohr–Coulomb strength envelope resting on a firm foundation. The second example is a simple slope described by Charles and Soares (1984) that is comprised of soil with a nonlinear Mohr–Coulomb strength envelope resting on a firm foundation. The third example is an end-of-construction, post-filling stability analysis of the downstream slope of Oroville Dam, a zoned embankment dam in California, described by Duncan et al. (2014). The shell and transition zone materials have separate nonlinear strength envelopes, while the core materials have linear strength envelopes. The latter two examples assume that a nonlinear failure envelope is required to provide a realistic representation of the soil behavior, as discussed in the sources.

In these examples, limit equilibrium analyses were performed using Spencer's (1967) method as implemented in Slide v7 (Rocscience 2016a), while the SSR analyses were performed using the finite element program RS2 v9 (Rocscience 2016b) and the two-dimensional finite difference program FLAC v8 (Itasca 2016). The built-in automatic strength reduction routines in the respective programs were used for strength reduction analyses, except for the MHB analyses performed in RS2. Since RS2 implements strength reduction for GHB materials using the approach proposed by Hammah et al. (2005), which is specific to rock materials, the MHB analyses in RS2 were manually performed using the routine described in this paper to define reduced MHB parameters for each *SRF*. Each MHB model was executed separately to define the highest *SRF* where the model converged. Non-convergence was assessed using absolute energy in RS2 for automatic SSR, normalized maximum displacement (Griffiths and Lane 1999) in RS2 for manual SSR, and unbalanced force in FLAC for all SSR analyses. All of the numerical analyses (finite element or finite difference) use non-convergence criteria that meet or exceed the suggestions of Griffiths and Lane (1999). Plots of maximum normalized displacement versus *SRF* from the manual SSR analyses in RS2 are provided in Figs. 3, 5 and 8 to show the transition to non-convergence. As the *SRF* increases, the calculated maximum displacement for models that converged exhibit a logical gradual rise, while the transition to non-convergence is abrupt. Thus, for the examples considered, the critical SRF is not strongly sensitive to the non-convergence criterion.

In all three examples, the Young's modulus and Poisson's ratio of all materials were taken to be equal to 100 MPa and 0.3, respectively. These values are consistent with the recommendations by Griffiths and Lane (1999) for use of the SSR method when project-specific elastic property values are not available. Non-associated plastic flow with zero dilation was considered in all analyses performed using RS2 and FLAC. The models were discretized using eight-node quadrilateral elements (RS2) or zones (FLAC). The models used relatively fine discretization to reduce the influence of mesh sensitivity. Because small deformations occurred up to the point of instability, excessive element deformation did not influence the calculated critical *SRF* values. The bottom horizontal boundaries were pinned, and vertical boundaries were represented using rollers.

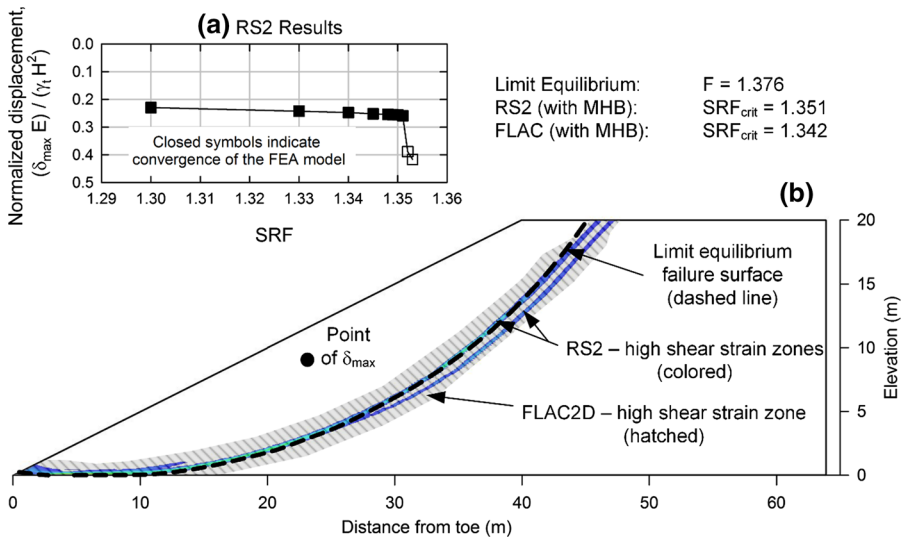

Fig. 3 Stability analysis comparison for simple 2H:1V soil slope—**a** *SRF* results and **b** failure mechanisms

5.1 Simple Slope with Linear Failure Envelope—Griffiths and Lane (1999)

The first validation case follows an example developed by Griffiths and Lane (1999) based on Bishop and Morgenstern (1960). The slope is 20 m high with an inclination of 2H:1V and the width of the crest from the top of the slope to the vertical model boundary is equal to 24 m. The homogeneous soil has a unit weight of 20 kN/m^3, $\phi' = 20°$, and $c = 20$ kPa. Pore pressures were assumed to be zero. Griffiths and Lane (1999) report a critical strength reduction factor of 1.35 for a mesh with 200 elements. Their result agrees closely with the non-circular limit equilibrium analysis result of $F = 1.38$ found using Spencer's method (1967).

A linear envelope can be modeled with MHB by using a value of b equal to or very close to 1.0. Although the MHB criterion is not needed for a linear failure envelope, this example helps to illustrate the utility and flexibility of the MHB criterion. The MHB parameters used to represent the full shear strength were $a = 1.0399$, $b = 0.9999$, and $t = 0.5634$ with the normalization stress set equal to $P_a = 101.3$ kPa.

The slope was modeled in RS2 and FLAC with both the linear Mohr–Coulomb model and the MHB parameters. The shear strength reduction results are displayed graphically in Fig. 3. A comparison of the results is provided in Table 1. The maximum displacement in the critical RS2 model occurred near the slope face about 9 m above the base and 23 m from the toe as indicated in Fig. 3.

The results presented in Table 1 indicate the MHB failure criterion is able to replicate the results of the commonly used and accepted Mohr–Coulomb method to greater resolution than the typical uncertainty in the shear strength parameters. The numerical analyses all predict a critical *SRF* within a range of 0.01 of each other. The numerical analyses also all predict slightly

Table 1 Results for 20-m slope with linear strength envelope

Method or source	Failure criterion	Number of elements or zones, *N*	Factor of safety or SRF_{crit} (% difference from LE)
Limit equilibrium (Spencer, non-circular)	Linear	–	1.38
Griffiths and Lane (1999)	Linear	200	1.35 (− 1.9%)
RS2 (automated routine)	Linear	15,000	1.34 (− 2.5%)
RS2 (manual routine)	MHB	15,000	1.35 (− 1.8%)
FLAC (automated routine)	Linear	5208	1.35 (− 2.2%)
FLAC (automated routine)	MHB	5208	1.34 (− 2.5%)

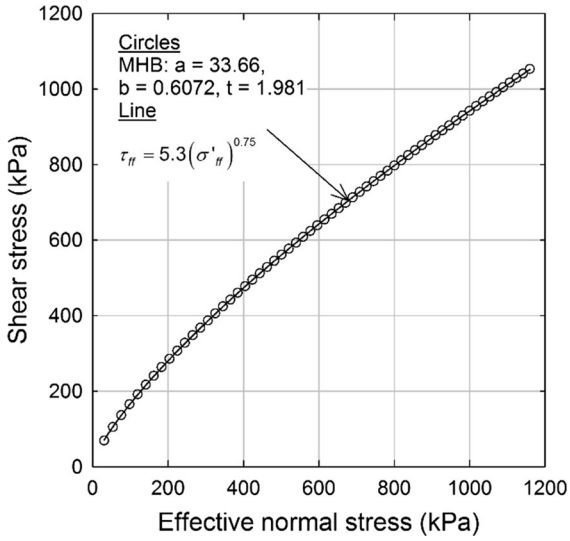

Fig. 4 Failure envelopes for good quality compacted slate (after Charles and Soares 1984)

lower *SRF* than the limit equilibrium factor of safety. However, all the results are within 2.5% of the limit equilibrium value. Figure 3 shows an excellent agreement between the failure mechanisms predicted by limit equilibrium and finite element analysis for this problem.

5.2 Stability of a Rockfill Slope—Charles and Soares (1984)

Charles and Soares (1984) present several examples of nonlinear shear strength envelopes for compacted rockfill. A soil labelled as heavily-compacted, good quality slate was stated to have a failure envelope described by a two-parameter power function with a coefficient of 5.3 and an exponent of 0.75. This power function is plotted as a solid line in Fig. 4. An MHB envelope was fit to match the power function using minor principal stresses ranging from 0.1 to 600 kPa. A large range was used to show that the MHB parameters can be found that match a power function over a wide range of effective normal stresses. The initial set of MHB parameters was found by numerically minimizing the area between the Charles and Soares power function and the equivalent failure envelope represented by the MHB equation.

Charles and Soares (1984) presented stability analysis results for their two-parameter power function in the form of a chart solution that plotted a stability number against the slope inclination (cot β). Their chart assumes a firm foundation and zero pore water pressure. Using their chart solution, the factor of safety for a 25 m high, 1.5H:1V slope of compacted slate with a total unit weight of 21 kN/m^3 is 2.99. Pore pressures were assumed to be zero. The slope was analyzed using limit equilibrium analysis with both circular and noncircular failure surfaces and SSR analysis using RS2 and FLAC. The width of the crest from the top of the slope to the vertical model boundary is equal to 30 m. The results are summarized in Table 2.

As shown in Table 2, the critical *SRF* values from the numerical analyses are 4–6% lower than the factor of safety from limit equilibrium. However, as indicated in Fig. 5, the two approaches do not find exactly the same failure mechanism, which may lead to the slightly different assessment of stability. The differences between the limit equilibrium and SSR results provided in Table 2 are similar to those reported by Tschuchnigg and Schweiger (2015) and Tschuchnigg et al. (2015). For linear failure envelopes, these researchers attributed the slightly lower SRF_{crit} from SSR to the effects of tensile zones in the numerical

Table 2 Results for 25-m slope with nonlinear strength envelope

Method or source	Failure criterion	Number of elements or zones, *N*	Factor of safety or SRF_{crit} (% difference from LE)
Charles and Soares (based on Bishop)	Power function	–	2.99
Limit equilibrium (Bishop, circular)	Power function	–	3.00
Limit equilibrium (Spencer, non-circular)	Power function	–	3.00
RS2 (manual routine)	MHB	15,000	2.82 (− 6.0%)
FLAC2D (automated routine)	MHB	8640	2.87 (− 4.3%)

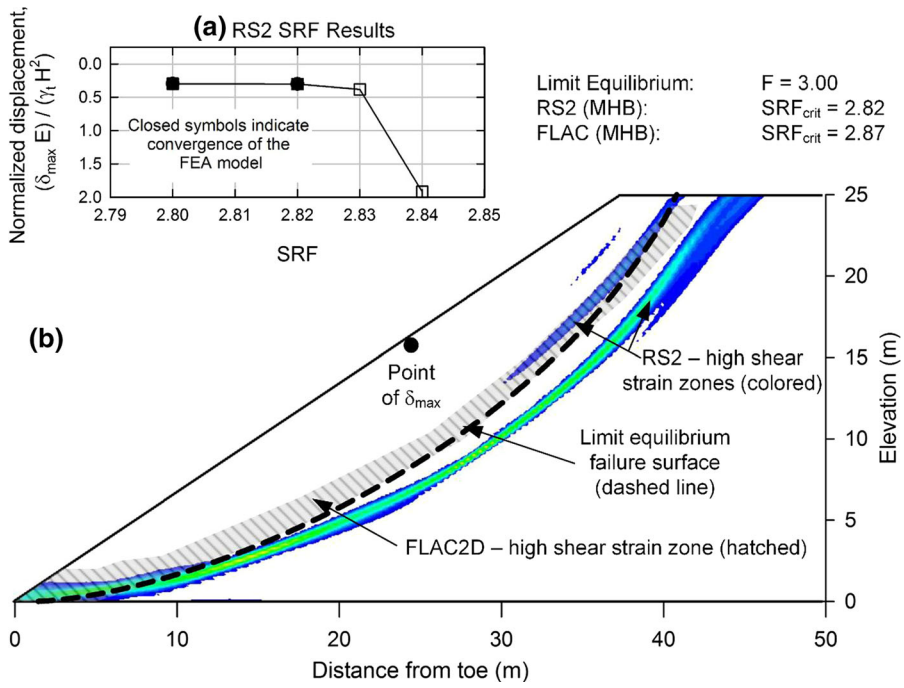

Fig. 5 Stability analysis comparison for 1.5H:1V slate rockfill slope—**a** *SRF* results and **b** failure mechanisms

models and the influence of the assumption regarding the dilation angle. The RS2 and FLAC results are less than 2% different, despite using different methods to factor the strength envelope. The maximum displacement in the critical RS2 model occurred slightly below the slope face about 16 m above the base.

5.3 Oroville Dam—Duncan et al. (2014)

The third example is Oroville Dam for which nonlinear limit equilibrium analyses were presented in Duncan et al. (2014). As depicted in Fig. 6, the dam has an inclined core with a transition zone and a rockfill shell. For the conditions after first filling, the full pool elevation is considered and applied to the highly permeable upstream shell and transition soils. The core materials were assigned total stress linear strength envelopes. Stability analyses of the downstream slope are dominated by the behavior of the shell, which exhibits nonlinear shear strength behavior. The transition zone also can be modeled by a nonlinear envelope.

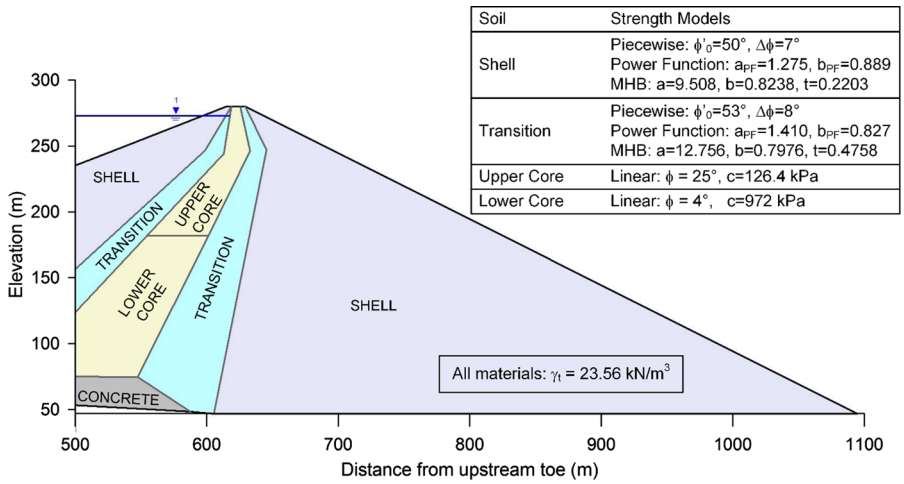

Fig. 6 Oroville Dam (after Duncan et al. 2014)

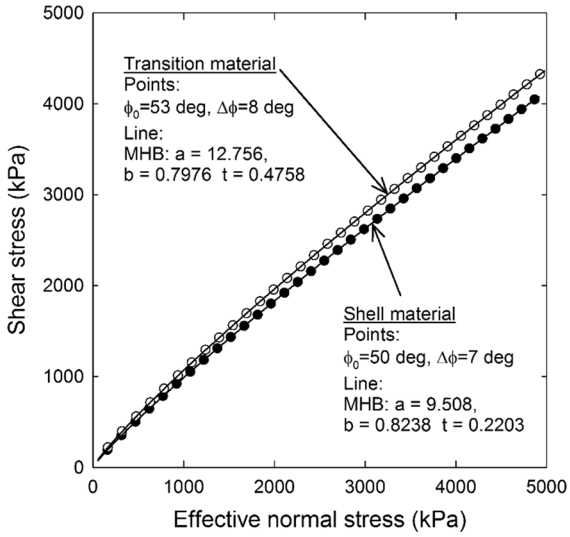

Fig. 7 Shell and transition soil failure envelopes for Oroville Dam

The nonlinear relationship between shear strength and normal stress are presented in Duncan et al. (2014) for both the shell and transition soils in terms of stress-dependent secant friction angles. Modified Hoek–Brown envelopes were fit to match these relationships for normal stresses up to 5000 kPa as shown in Fig. 7.

The slope was analyzed using limit equilibrium analysis with noncircular failure surfaces and SSR analysis using RS2 and FLAC. The MHB parameters were adjusted for each *SRF* as described previously. The shear strength of the low permeability clay core was modeled using a Mohr–Coulomb criterion and was also adjusted for each step of the strength reduction analysis. As shown in Table 3, the critical *SRF* values from the numerical analyses are 4–5% lower than the factor of safety from limit equilibrium. However, as indicated in Fig. 8, the two approaches do not find exactly the same failure mechanism, which may lead to the slightly different assessment of stability. The RS2 and FLAC results are less than 1% different, despite using different methods to factor the strength envelope. The maximum displacement in the critical RS2 model occurred at the slope face 656 m from the upstream toe and at elevation 267.6 m.

As shown in Fig. 8, the critical noncircular failure surface from the current LE analysis and the critical circular surface found by Duncan et al. (2014) are not the same; however, both analyses yield the same factor of safety. The critical failure surfaces from both LE analyses are superimposed on the maximum shear strain contours from the SSR analyses. While the general location and shape of the LE failure surfaces agree with the locations of high maximum shear strain, the numerical analyses identify a more complex failure mechanism, including shear strain in the low permeability core (upper left of Fig. 8b). The vertically inclined zones of the dam experience a mechanism similar to toppling with high shear strain at the boundaries between the zones. The near orthogonal orientation of these secondary shear zones to the critical failure surface is the result of the zone geometry. These complexities are likely the cause of the lower strength reduction factor compared to the LE analyses and cannot be readily represented by a LE failure mechanism.

6 Discussion

The first example showed that an MHB envelope can be used to effectively model the stability of a simple example slope presented in Griffiths and Lane (1999). This example uses a linear failure envelope which illustrates the flexibility of the MHB criterion for both linear and nonlinear envelopes. Numerical analyses of this example used both finite element and finite

Table 3 Results for Oroville Dam with multiple soils having linear and nonlinear strength envelopes

Method or source	Failure criterion	Number of elements or zones, *N*	Factor of safety or SRF_{crit} (% difference from LE)
Duncan et al. (2014)	Piecewise linear	–	2.16
Limit equilibrium (Spencer, non-circular)	Two parameter power functions	–	2.16
RS2 (manual routine)	MHB	17,398	2.06 (− 4.6%)
FLAC2D (automated routine)	MHB	43,875	2.08 (− 3.7%)

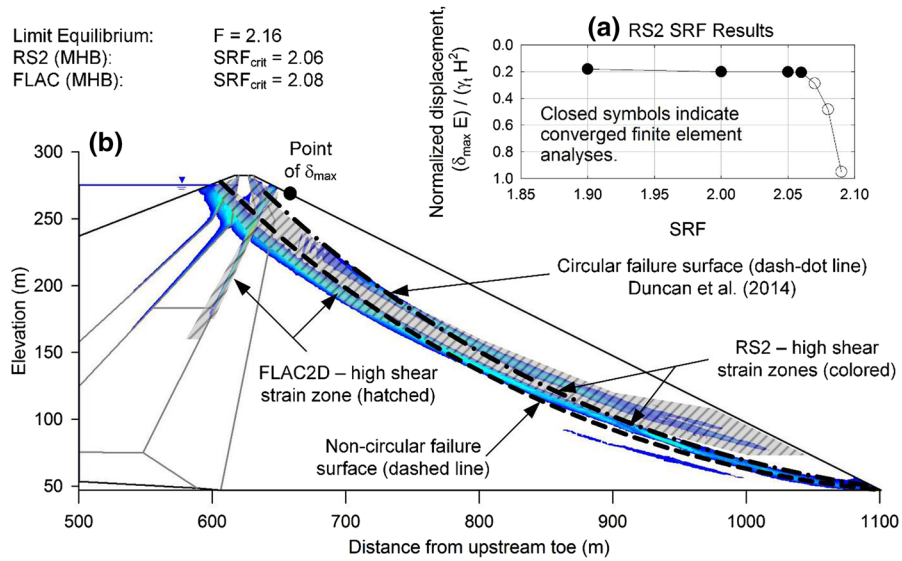

Fig. 8 Strength reduction analysis results for Oroville Dam example

difference schemes and found close agreement (less than 2.5% difference) with each other and with the comparison limit equilibrium analysis.

The second example used a chart solution developed by Charles and Soares (1984) for steep, rockfill slopes with nonlinear failure envelopes. The strength reduction analyses were performed with both finite element and finite difference methods. The critical *SRF* predicted by both methods was within 5% of the limit equilibrium values. This example showed the application of MHB to model slopes in soils with nonlinear failure envelopes.

The third example examined the real-world example of the downstream face of Oroville Dam. Two of the three soil zones were modeled using the MHB criterion. The resulting match with limit equilibrium was very close (less than 5% difference). This example illustrates that MHB can be applied to real slopes with complex geometry and multiple zones.

In general, the critical *SRF* values predicted using the MHB failure criterion matched or were slightly lower than limit equilibrium analysis of the similar problem. The strength reduction analyses with the linear envelope and MHB were very close in the first example. This suggests that the differences between the limit equilibrium and MHB results are caused by differences in the use of limit equilibrium compared to numerical methods to evaluate stability, rather than any inadequacy of the MHB approach to model soil behavior.

7 Conclusions

The Generalized Hoek–Brown failure criterion was developed to model rock behavior. However, the combination of the nonlinearity of this model and its basis on principal stresses makes it attractive as failure criterion for soil as well. The GHB criterion is available in the most common commercial numerical analysis software packages.

This paper has presented a modified approach to using the Generalized Hoek–Brown that uses atmospheric pressure rather than the unconfined compressive strength as a normalization stress. The parameters that define the inclination, a; curvature, b, and tensile intercept, t, for the soil can be determined from triaxial test data (VandenBerge et al. 2018). These parameters, along with $\sigma'_{ci} = P_a$, can be used directly in numerical analysis.

Numerical strength reduction analysis is performed by reducing the failure criterion incrementally until the numerical model fails to converge. Unlike linear models, the MHB failure criterion cannot be reduced by directly dividing the parameters by the *SRF*. A numerical scheme was proposed to fit a new set of MHB parameters to each reduced failure envelope. This method is similar to that suggested by Hammah et al. (2005). However, different parameters are adjusted because the MHB approach does not assume the material is rock.

Analytical evaluation of a supported vertical cut validates the use of MHB for soil in the simple linear case. Three examples of increasing complexity illustrated that the MHB approach can be used successfully with shear strength reduction analysis to evaluate slope stability. The critical strength reduction factors tended to be a few percent lower than the corresponding limit equilibrium analyses for numerical analyses with either linear or MHB envelopes.

References

Baker R (1980) Determination of the critical slip surface in slope stability computations. Int J Numer Anal Methods Geomech 4:333–359

Bishop AW, Morgenstern NR (1960) Stability coefficients for earth slopes. Géotechnique 10:129–150

Castellanos BA, Brandon TL, VandenBerge DR (2016a) Correlations for fully softened shear strength parameters. Geotech Test J 39:568–581

Castellanos BA, Brandon TL, VandenBerge DR (2016b) Use of fully softened shear strength in slope stability analysis. Landslides 13:697–709

Charles JA, Soares MM (1984) Stability of compacted rockfill slopes. Géotechnique 34:61–70

Chen X, Ren J, Wang D, Lyu Y, Zhang H (2018) A generalized strength reduction concept and its applications to geotechnical stability analysis. Geotech Geol Eng. https://doi.org/10.1007/s10706-018-00765-1

Cheng YM (2003) Location of critical failure surface and some further studies on slope stability analysis. Comput Geotech 30(1):255–267

Cheng YM, Lansivaara T, Wei WB (2007) Two-dimensional slope stability analysis by limit equilibrium and strength reduction methods. Comput Geotech 34:137–150

Ching JC, Phoon KK, Hu YG (2010) Observations on limit equilibrium-based slope reliability problems with inclined weak seams. J Eng Mech 136:1220–1233

Dawson E, You K, Park Y (2000) Strength-reduction stability analysis of rock slopes using the Hoek–Brown failure criterion. In: Proceedings of GeoDenver 2000, pp 65–77

Duncan JM, Wright SG, Brandon TL (2014) Soil strength and slope stability, 2nd edn. Wiley, New York

Fu W, Liao Y (2010) Non-linear shear strength reduction technique in slope stability calculation. Comput Geotech 37:288–298

Greco VR (1996) Efficient Monte Carlo technique for locating critical slip surface. J Geotech Eng 122:517–525

Griffiths DV, Lane PA (1999) Slope stability analysis by finite elements. Géotechnique 49:387–403

Hammah RE, Yacoub TE, Corkum BC, Curran JH (2005) The shear strength reduction method for the generalized Hoek–Brown criterion. In: Proceedings of 40th US Symposium Rock Mechanics (USRMS). American Rock Mechanics Association, 6 pp

Hoek E, Brown ET (1980) Empirical strength criterion for rock masses. J Geotech Eng 106:1013–1035

Hoek E, Carranza-Torres C, Corkum BC (2002) Hoek–brown failure criterion—2002 edition. In: Proceedings of 5th North American rock mechanics symposium NARMS-TAC 267–73

Itasca (2016) Fast lagrangian analysis of continua version 8. Itasca Consulting Group Inc., Minneapolis

Jiang JC, Baker R, Yamagami T (2003) The effect of strength envelope nonlinearity on slope stability computations. Can Geotech J 40:308–325

Ledesma O, Garcia Mendive I, Sfriso A (2016) Factor of safety by the strength-reduction technique applied to the Hoek–Brown model. In: ENIEF 2016, Argentina

Lee YK, Bobet A (2014) Instantaneous friction angle and cohesion of 2-D and 3-D Hoek–Brown rock failure criteria in terms of stress invariants. Rock Mech Rock Eng 47:371–385

Lee KL, Seed HB (1967) Drained strength characteristics of sands. J Soil Mech Found Div 93:117–141

Leshchinsky B, Ambauen S (2015) Limit equilibrium and limit analysis: comparison of benchmark slope stability problems. J Geotech Geoenviron Eng 141:04015043

Marachi ND, Chan CK, Seed HB (1972) Evaluation of properties of rockfill materials. J Soil Mech Found Div 98:95–114

Mesri G, Shahien M (2003) Residual shear strength mobilized in first-time slope failures. J Geotech Geoenviron Eng 129:2–31

Navin MP, Filz GM (2006) Numerical stability analyses of embankments supported on deep mixed columns. In: GeoChanghai international conference, Shanghai, China

Pockoski M, Duncan JM (2000) Comparison of computer programs for analysis of reinforced slopes. Center for Geotechnical Practice and Research, Virginia Tech, Blacksburg, p 150

Rocscience (2016a). Slide v7.0-2D limit equilibrium slope stability analysis. Rocscience, Inc., Toronto

Rocscience (2016b). RS2-Finite element analysis for excavations and slopes. Rocscience, Inc., Toronto

Shen J, Karakus M, Xu C (2012) Direct expressions for linearization of shear strength envelopes given by the generalized Hoek–Brown criterion using genetic programming. Comput Geotech 44:139–146

Shukha R, Baker R (2003) Mesh geometry effects on slope stability calculation by FLAC strength reduction method—linear and non-linear failure criteria. In: Proceedings of 3rd international FLAC symposium, Sudbury, Canada, pp 109–116

Spencer E (1967) A method of analysis of the stability of embankments assuming parallel interslice forces. Géotechnique 17:11–26

Tschuchnigg F, Schweiger HF (2015) Performance of strength reduction finite element techniques for slope stability problems. In. Proceedings of XVI ECSMGE geotechnial engineering for infrastructure and development, pp 1687–1692

Tschuchnigg F, Schweiger HF, Sloan SW, Lyamin AV, Raissakis I (2015) Comparison of finite-element limit analysis and strength reduction techniques. Geotechnique 65:249–257. https://doi.org/10.1680/geot.14.P.022

VandenBerge DR, Duncan JM, Brandon TL (2013) Fully softened strength of natural and compacted clays for slope stability. In: Geo-congress 2013, stab perform slopes embankments III, pp 221–233

VandenBerge DR, McGuire MP, Castellanos BA (2018) Linear and nonlinear effective stress shear strength envelopes from triaxial test data. Center for Geotechnical Practice and Research, Virginia Tech, Blacksburg, p 57

VandenBerge DR, Castellanos BA, McGuire MP (2019) Comparison and use of failure envelopes for slope stability. Geotech Geol Eng. https://doi.org/10.1007/s10706-018-0742-1

Xie Y, Leshchinsky B (2016) Active earth pressures from a log-spiral slip surface with arching effects. Geotech Lett 00:00. https://doi.org/10.1680/jgele.16.00015